Theoretical study of the hydrogen release mechanism from a lithium derivative of ammonia borane, LiNH 2BH 3–NH 3BH 3

ARTICLE *in* CHEMICAL PHYSICS LETTERS · NOVEMBER 2011

Impact Factor: 1.9 · DOI: 10.1016/j.cplett.2011.10.010

3 AUTHORS, INCLUDING:

Nguyen Vinh Son
University of Leuven
35 PUBLICATIONS **490** CITATIONS
SEE PROFILE

Minh Tho Nguyen
University of Leuven
748 PUBLICATIONS **10,861** CITATIONS
SEE PROFILE

Chemical Physics Letters 517 (2011) 22–28

Contents lists available at SciVerse ScienceDirect

Chemical Physics Letters

journal homepage: www.elsevier.com/locate/cplett

Theoretical study of the hydrogen release mechanism from a lithium derivative of ammonia borane, $LiNH_2BH_3$–NH_3BH_3

Saartje Swinnen [a], Vinh Son Nguyen [a,b], Minh Tho Nguyen [a,*]

[a] Department of Chemistry, Katholieke Universiteit Leuven, B-3001 Leuven, Belgium
[b] Faculty of Chemistry, and Center for Computational Science, National University of Education, Hanoi, Viet Nam

ARTICLE INFO

Article history:
Received 12 March 2011
In final form 7 October 2011
Available online 12 October 2011

ABSTRACT

Ammonia borane and lithium amidoborane proved to have potential as efficient hydrogen storage materials. Although a combination of both compounds, $LiNH_2BH_3$–NH_3BH_3 has been shown to have even better hydrogen release characteristics, the inherent process was not clear. We determined the reaction mechanism of H_2 release from $LiNH_2BH_3$–NH_3BH_3 using computational quantum chemistry methods (MP2 and CCSD(T) methods and aug-cc-pVnZ basis sets). The energy barrier for H_2 release becomes lower than in pure $LiNH_2BH_3$ or NH_3BH_3 in agreement with experiment. Relevant transition structures are analyzed in detail and the initial formation of a cyclic adduct is likely responsible for the strong reduction of energy barriers.

1. Introduction

Hydrogen is considered as an alternative for the extensive fossil fuel usage [1,2]. However there are still some challenges including its storage and production, which need to be resolved before a 'hydrogen economy' could emerge. The storage of hydrogen for use in transportation remains a major concern due to its low volumetric density (8 MJ/L for liquid hydrogen compared to gasoline 32 MJ/L). Ammonia borane (NH_3BH_3, **ab**) has the potential of meeting the goals set by the USA Department of Energy (DOE) [3]. It is a white crystalline solid at room temperature and has a hydrogen content of ~19.6 wt.% [4–8]. Ammonia borane releases H_2 according to the following reactions:

$$n(NH_3BH_3) \rightarrow n(NH_2BH_2) + nH_2 \quad (1)$$

$$(NH_2BH_2)_n \rightarrow (NHBH)_n + nH_2 \quad (2)$$

$$(NHBH)_n \rightarrow (NB)_n + nH_2 \quad (3)$$

where $(NHBH)_n$ can be formed as different compounds like polyiminoborane, borazine, polyborazine, cross-linked materials, etc. Reaction (1) occurs in a temperature range of 70–130 °C depending on the heating rate, whereas reaction (2) is carried out between 110 and 200 °C, and reaction (3) above 1200 °C. The reaction pathways of hydrogen release from **ab**, and its dimer $(\mathbf{ab})_2$ were studied by many groups [9–15]. Theoretical studies using high accuracy computational quantum chemistry methods showed that the energy barrier for hydrogen release from the **ab** monomer without any catalyst is 36 kcal/mol (CCSD(T)/CBS), which is higher than the B–N dissociation energy of ~25 kcal/mol [16,17]. Subsequent calculations pointed out that after dissociation, the BH_3 fragment can act as a catalyst yielding an energy barrier of ~6 kcal/mol for producing one H_2 molecule. For the dimer $(\mathbf{ab})_2$, calculated results revealed an energy barrier of at least 44 kcal/mol for the release of one H_2 molecule. Formation of the diammoniate of diborane ion pair isomer, DADB, which proved to be important in the hydrogen production from **ab** [18–20], requires to overcome an energy barrier of 28.1 kcal/mol. From the dimeric DADB form, two hydrogen molecules can be released with energy barriers <20 kcal/mol. Intensive search has been carried out with the aim to find a way of further lowering the energy barrier of reaction (1), and thereby the decomposition temperature.

Xiong et al. [21] substituted one H of the NH_3 moiety by the more electron donating elements Li and Na. These authors found that lithium amidoborane (**liab**) and sodium amidoborane tend to improve the energetics, but have different dehydrogenation characteristics with respect to **ab** itself. Lithium and sodium amidoboranes were prepared by ball milling 1:1 M ratios of **ab** and the corresponding alkali-metal hydrides are prepared according to the reactions (4) and (5):

$$NH_3BH_3\,(s) + LiH\,(s) \rightarrow LiNH_2BH_3 + H_2\,(g) \quad (4)$$

$$NH_3BH_3\,(s) + NaH\,(s) \rightarrow NaNH_2BH_3 + H_2\,(g) \quad (5)$$

Subsequently, $LiNH_2BH_3$ releases H_2 directly on heating at temperatures around 92 °C with no emission of borazine. This route represents an advantage over NH_3BH_3 which releases H_2 at 108–154 °C with production of a small amount of borazine. Within 1 h about 8 wt.% hydrogen is released from $LiNH_2BH_3$ as follows:

* Corresponding author. Fax: +32 16 32 79 92.
E-mail address: minh.nguyen@chem.kuleuven.be (M.T. Nguyen).

0009-2614/$ - see front matter © 2011 Elsevier B.V. All rights reserved.
doi:10.1016/j.cplett.2011.10.010

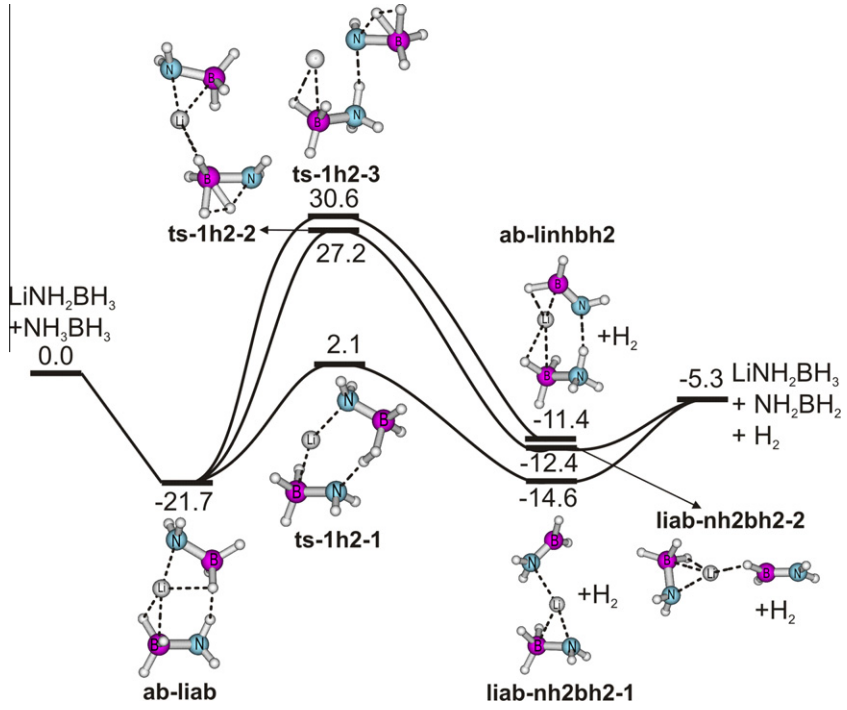

Figure 1. Schematic minimum energy pathways for the release of the first H_2 from **ab**–**liab**. Relative energies given in kcal/mol are obtained from MP2/aVTZ + ZPE calculations.

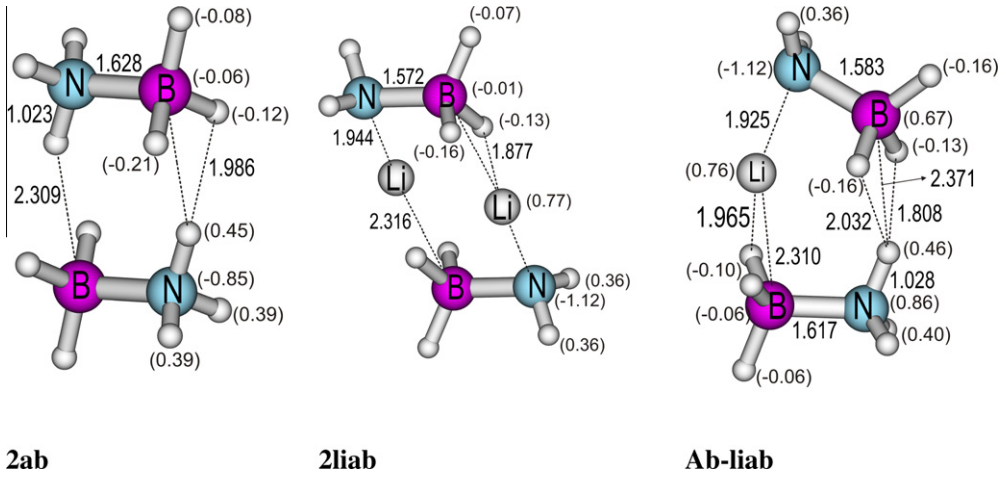

Figure 2. Structural parameters obtained from MP2/aVTZ calculations for the complexes of **2ab**, **2liab** and **ab**–**liab**. Bond lengths are given in angstrom and bond angles in degree.

$$n\mathrm{LiNH_2BH_3} \rightarrow (\mathrm{LiNBH})_n\,(\mathrm{s}) + 2n\,\mathrm{H_2}\,(\mathrm{g}) \quad (6)$$

The reaction pathway associated with reaction (4) was studied earlier in detail by our group [22]. Our results showed a two-step mechanism for H_2 release from the monomer. In the first step, hydrogen of boron is transferred to lithium with an energy barrier of ~32 kcal/mol (results at the CCSD(T)/aug-cc-pVTZ level of theory). This step is followed by H_2 formation with a low energy barrier of only ~4 kcal/mol. For the dimer, we again found a two-step mechanism in which the first step involves the transfer of one H of boron to lithium with an energy barrier of ~48 kcal/mol. The reason for this relatively higher energy barrier can be found in the formation of a very stable complex between the two **liab** molecules. The energy barrier for H_2 release amounts then to ~12 kcal/mol.

More recently, Wu et al. [23] carried out experimentally a condensation of the two components, **ab** and **liab**, into a **ab**–**liab** adduct, and studied the hydrogen release reactions. The experimental results showed that the new component release 14.0 wt.% of H_2 in a stepwise manner with peak temperatures at ca. 80–140 °C, respectively. Borazine and aminoborane were not detectable. More recently, Li et al. [24] performed a theoretical study on the **ab**–**liab** compound and suggested a H_2 release via a combination of the hydric $H^{\delta-}$(B) from **liab** and the protonic $H^{\delta+}$(N) form **ab** rather than from the **liab** or **ab** layer alone. However the reaction mechanism with the relevant transition structures for such process was not established. In this context, we set out to investigate the detailed H_2 release from $LiNH_2BH_3$–NH_3BH_3 using high level electronic structure calculations. We not only construct the relevant potential

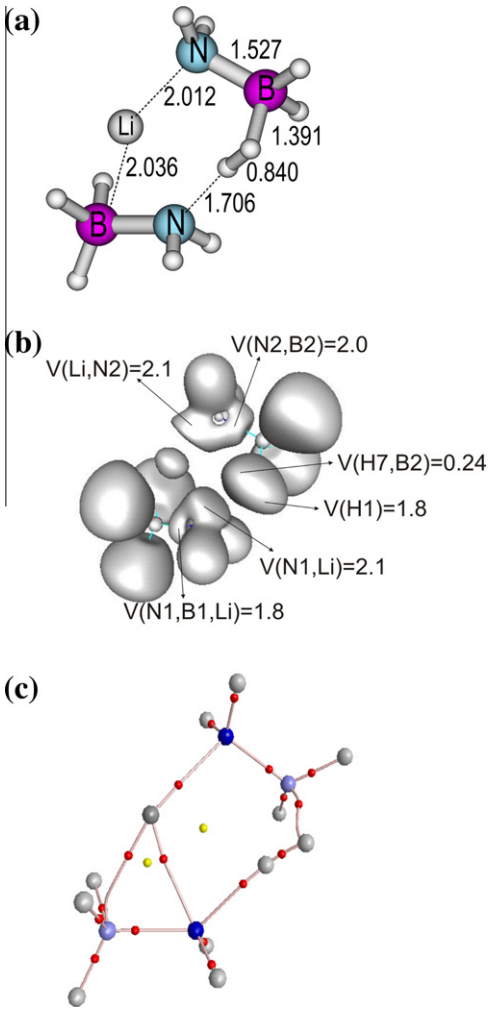

Figure 3. Structure analysis of **ts-1h2-1**: (a) selected geometrical parameters, (b) ELF basins including populations of some important basins, (c) AIM map. All analyses are based on MP2/aVTZ optimized structure.

energy profiles for the release of one H_2 but also the pathways for the release of the second and the third H_2 molecules. In addition we analyze the electronic characteristics of the favored reaction pathways in order to gain a better understanding of the reaction mechanism.

2. Computational methods

All electronic structure calculations are carried out using the Gaussian 09 [25] and Molpro-2006 [26] suites of programs. Geometrical parameters, vibrational frequencies and zero point energies (ZPE) of the stationary points are initially calculated at the second-order perturbation theory (MP2) [27] using the correlation consistent aug-cc-pVDZ basis-set [28–30] (denoted hereafter as aV*n*Z, with $n = D$, T and Q). The geometrical parameters of the relevant equilibrium and transition (TS) structures are then refined using a larger basis set, namely at the MP2/aVTZ level. The zero point energies are scaled by a factor 0.97 from the MP2/aVDZ vibrational frequencies as described in a previous study [17]. All potential energy profiles considered are initially mapped out using the MP2/aVTZ energies with appropriate ZPE corrections. To obtain more accurate relative energy values we perform single-point energy calculations using the coupled-cluster CCSD(T) method [31,32] in conjunction with the aVTZ basis set on the MP2/aVTZ optimized energy minima and transition structures. In all MP2 and CC calculations, the core orbitals are kept frozen. To ensure that a transition structure is correctly connecting the right energy minima, we carry out the intrinsic reaction coordinate (IRC) calculations [33] at the MP2/aVDZ level.

In attempt to understand more about the electron redistribution along the reaction pathways, we perform an analysis of the electronic populations of some important structures using the atom-in-molecule (AIM) and electron localization function (ELF) approaches. In the AIM approach, we endeavor to find the critical points (CPs) [34,35], that are defined by the AIM theory as the points where the gradient of the electron density becomes zero. There are two important types of CPs, namely, a (3,−1) point or a bond critical point which defines a chemical bond, and a (3,+1) point or a ring critical point which denotes the formation of a ring within a molecule. We use the MP2/aug-cc-pVTZ electron densities for the AIM analysis. The CPs and bond paths are calculated with the Aim2000 program package [35].

The ELF theory partitions a total electron density into electron basins (Ω_i) [36]. Two types of basins can exist, including core basins, which are located around the nuclei, and the valence basins describing the bonding. The integral (7) of the electron density over Ω_i yields the population of a given basin:

$$N_i = \int_{\Omega i} \rho(r) dr \tag{7}$$

where r represents the space coordinates.

We use the Topmod program [37] to determine the ELF basins of the located equilibrium structures and important transition structures. The ELF isosurfaces are plotted using the graphical program gopenmol [38]. It is clear that the energetic and electronic characteristics derived correspond to the gas phase conditions of the species considered.

3. Results and discussion

3.1. Pathway for the release of the first H_2 molecule

The pathways associated with this process are schematically illustrated in Figure 1. Accordingly, the hydrogen release starts with formation of a complex **ab–liab** between NH_3BH_3 (**ab**) and $LiNH_2BH_3$ (**liab**). **ab–liab** has a relative energy of −21.7 kcal/mol with respect to **liab** + **ab**. The structure is comparable to the structures of the dimer of **ab** and the dimer of **liab** previously studied by us [17,22] (cf. Figure 2). The geometries of the three complexes located are similar to each other. The distances between the boron of one monomer and the H or Li connected to nitrogen of the other monomer are more or less the same for **2ab** and **2liab** and amount to 2.309 and 2.316 Å, respectively. In **ab–liab** the B···Li distance of 2.310 Å is similar however the B···H distance of 2.371 Å is slightly longer. The major difference in these complexes is their stability. **2ab** is thus relatively more stable compared to the two monomers, being −14.0 kcal/mol (results at CCSD(T)/aVTZ + ZPE). Let us mention that the dimeric structure **2ab** is the same as the structure previously reported and denoted as **dim** in Ref. [17]. Their Cartesian coordinates are now given in the Supplementary Information file.

Table 1
Relative energies (in kcal/mol) of the initial complex, TS and product of the reaction **ab** + **liab** calculated at three different levels of theory.[a]

System	MP2/pVTZ	CCSD(T)/pVDZ	CCSD(T)/pVTZ
ab + **liab**	0.0	0.0	0.0
Complex **ab–liab**	−21.7	−22.4	−21.7
ts-1h2-1	2.1	2.2	2.8
Complex **liab–nh$_2$bh$_2$-1**	−14.6	−14.2	−14.3

[a] CCSD(T) calculations are single point energy calculations based on MP2/aVTZ optimized structures. All values are corrected for ZPE contributions.

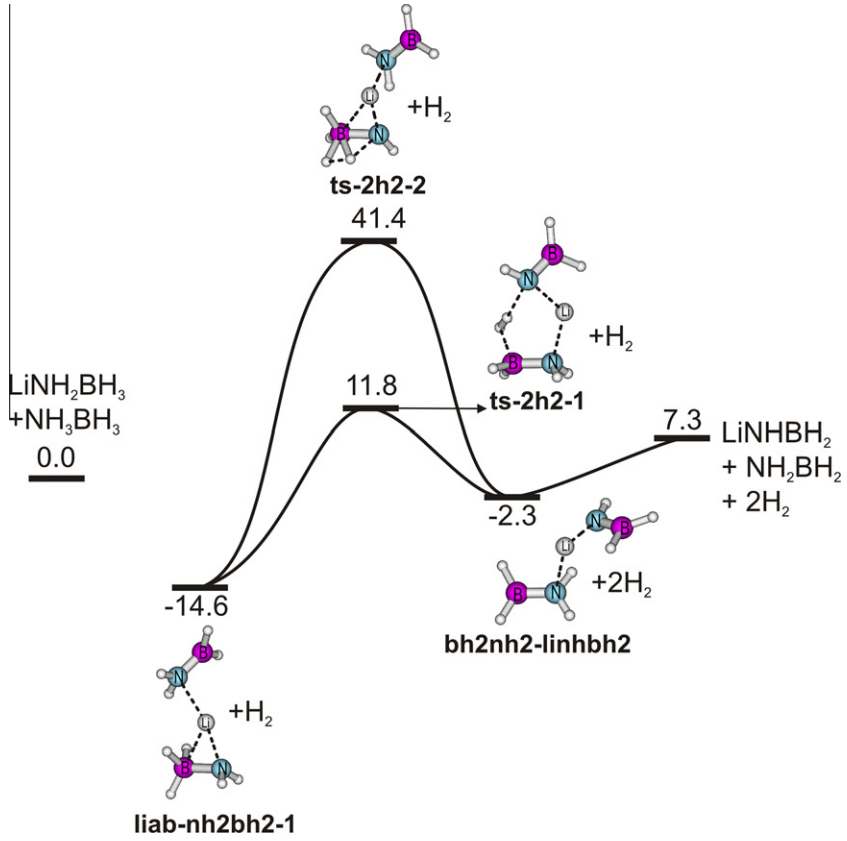

Figure 4. Schematic minimum energy pathways for the release of the second H_2 from **ab**–**liab**. Relative energies given in kcal/mol are obtained from MP2/aVTZ + ZPE calculations.

Introduction of Li in **ab** stabilizes **2liab** considerably, being −35.9 kcal/mol compared to the two monomers **liab**. The reason for this can be found in the charge distribution. The NBO populations are given in Figure 2 (numbers given in brackets). In this case, it is clear that Li will be more positive than a H at the same place. This will induce a larger charge difference between the H(B) and the H(N) or Li(N) of 0.6 and 0.8 electron, respectively, and such polarization results in a shorter distance between them, namely 1.986 Å for **2ab** and 1.877 Å for **2liab**. The high energy barriers for H_2 release can partially be understood by this stability as well. In the case of **2ab**, an energy barrier of 44.5 kcal/mol emerges because the corresponding TS is not stabilized.

With **2liab** an equally high energy barrier of 48.3 kcal/mol occurs because now the complex is more stable, and more energy is needed to change the structure of the complex. However, the relative energy as compared to the two monomers **2liab** is considerably lower, being 12.4 kcal/mol compared to 30.5 kcal/mol for **2ab**, because the associated TS is stabilized by Li. Another reason for the high energy barrier in the case of **2liab** is that nowhere in the complex, two hydrogen atoms interact already with each other such as the case with **2ab**. In **2ab**, an H(B) forms a dihydrogen bridge with an H(N) from the other **ab** molecule. In **2liab**, such kind of interaction does not exist. In **ab**–**liab**, only one H is actually substituted by one Li. This yields a complex which combines both advantages discussed above: including the lithium stabilizes the complex (but not so much, at −21.7 kcal/mol) and still one dihydrogen bond is already formed in the complex. This will result in a lower energy barrier which will be discussed below.

Starting from **ab**–**liab**, three different transition states (TS) for hydrogen release are located. In **ts-1h2-2** and **ts-1h2-3**, hydrogen release occur from the **ab** monomer and **liab**, respectively. This means that a H from borane interacts with a hydrogen(N) of the same molecule (**ab** or **liab**). **ts-1h2-2** leads to an energy barrier of 48.9 kcal/mol, and results in **liab–nh2bh2-2** as product, with a reaction energy of −12.4 kcal/mol. **ts-1h2-3** corresponds to a higher energy barrier of 52.3 kcal/mol and results in **ab–linhbh2** with a reaction energy of −11.4 kcal/mol.

A lower energy barrier can be found in **ts-1h2-1**, that is 23.8 kcal/mol, when H(B) of **liab** interacts with H(N) of **ab**. This lower barrier height can easily be explained from the fact that the largest charge difference (0.8 electron) occurs between those two hydrogens. A more detailed analysis of this TS can be found in Figure 3. Figure 3a–c depict some structural parameters, ELF isosurfaces with the electron populations of some relevant basins and the AIM map, respectively. In the TS, the leaving H atoms are already very close to each other, being 0.840 Å, suggesting that H_2 is almost completely formed. It seems that the positively charged H is nearly dissociated from N, while the negatively charged H is still connected to B. This picture can also be seen the ELF populations in which the V(H1) basin possesses a population of 1.8 electrons (Figure 3b). This basin has no influence of N anymore. Basin V(H7,B2) with a population of 0.24 electron still has some influence of B, even though it is almost empty, which suggests that H_2 is almost completely formed.

Perhaps more interesting to note is the fact that both N atoms have an interaction with Li, namely the basins V(N1,Li) and V(Li,N2) have populations of ∼2.1 electrons each. This suggests formation of a bond between Li and both N atoms. This can also be seen in the AIM map where a bond critical point is found between Li and the two Ns.

The AIM map in addition shows two ring critical points, which imply formation of two rings, including a three-membered and a six-membered ring. Nevertheless, each of the minimum **ab–liab** and TS **ts-1h2-1** apparently contains a loose seven-membered ring.

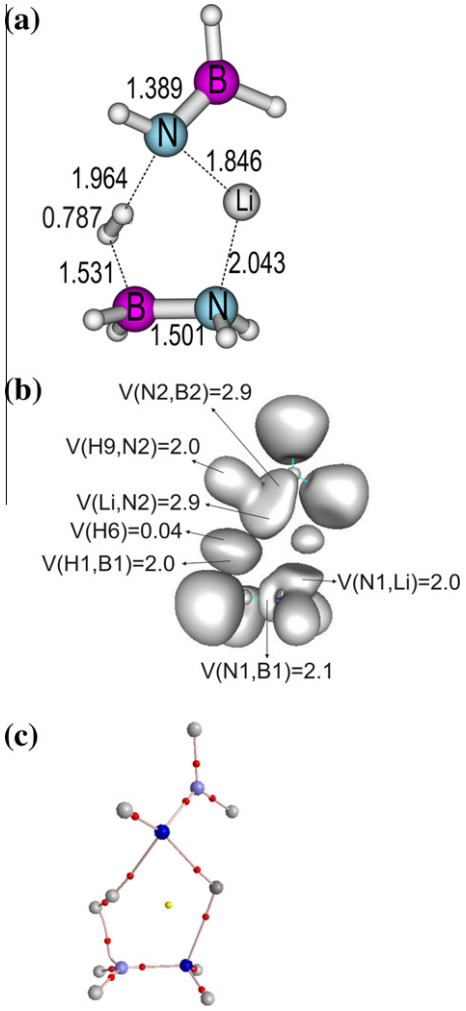

Figure 5. Structure analysis of **ts-2h2-1**: (a) selected geometrical parameters, (b) ELF basins including populations of some important basins, and (c) AIM map. All analyses are based on MP2/aVTZ optimized structure.

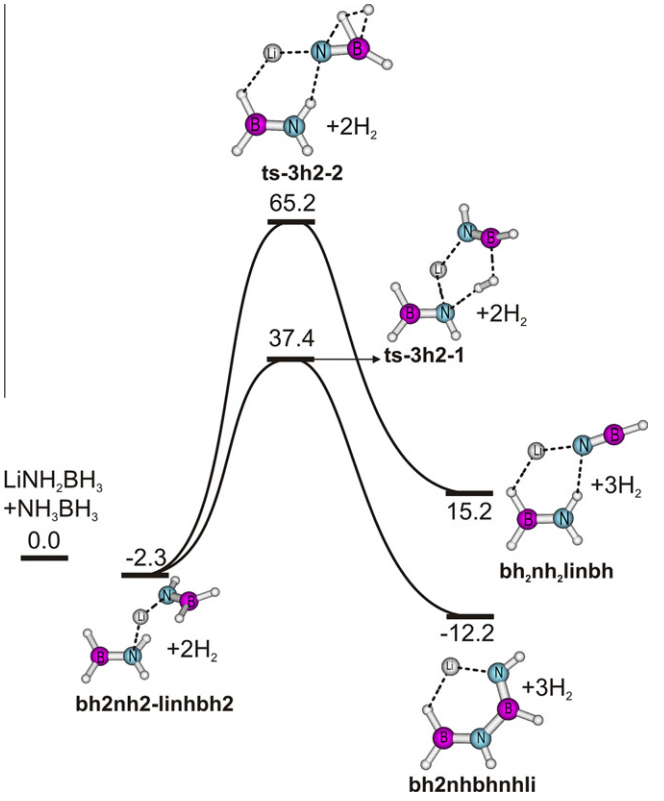

Figure 6. Schematic minimum energy pathways for the release of the third H_2 from **ab–liab**. Relative energies given in kcal/mol are obtained from MP2/aVTZ + ZPE calculations.

The presence of these cyclic forms that have lower ring strain tends to stabilize the complexed structure more effectively through new and partial bonds, and thus correlates with the finding that both the relevant complex and TS are stabilized.

The latter TS leads again to the formation of a complex between NH_2BH_2 and **liab**, namely **liab–nh2bh2-1**, with a relative energy of −14.6 kcal/mol. Due to the much lower energy barrier of the channel via **ts-1h2-1**, we expect that this TS occurs as the determining step, and thus the starting point for the release of the second hydrogen will be **liab–nh2bh2-1**. As mentioned above, results obtained from our electronic structure calculations are only valid for gas phase systems. However, on the basis of the reported experiments [21,23], we would suggest that in the case that a solid–gas equilibrium of the starting materials could initially be established following heating, a H_2 release could then occur in the gas phase, and the present calculated mechanism could be applied. If the starting materials are solid, and the H_2 release also occurs in this phase, our results cannot be applied, and appropriate treatments need to be considered.

3.2. Comparison between MP2 and CCSD(T) energy results

As for a further calibration of the calculated relative energies obtained using MP2/aVTZ method, we perform the coupled-cluster CCSD(T)/aVTZ single point energy calculations for the lowest pathway for one H_2 release. The results are summarized in Table 1. The relative energies obtained by different methods are similar to each other, with a relative energy difference of, at most, 0.7 kcal/mol. Due to limitations of our computational resources, we therefore only consider the MP2/aVTZ + ZPE calculations for the other reaction pathways bearing in mind an error of ±1.0 kcal/mol with respect to the CCSD(T)/aVTZ single point energy results.

3.3. Pathway for release of the second H_2 molecule

The energy profiles illustrating these processes are displayed in Figure 4. Starting from **liab–nh2bh2-1**, two TS's for H_2 release are found. The TS for H_2 release from the monomer LiAB, **ts-2h2-2**, is characterized with a high energy barrier of 56.0 kcal/mol. However a lower energy barrier can be found when $H(NH_2)$ of the NH_2BH_2 interacts with H from $-BH_3$ group of **liab**. This in fact occurs in **ts-2h2-1** whose energy barrier is reduced to 26.4 kcal/mol. Figure 5a–c summarize some related structural parameters, ELF isosurfaces with the electron populations and the AIM graphic map, respectively. In this case, the distance between the leaving Hs is only 0.787 Å suggesting that H_2 is completely formed at the TS. This view is further confirmed by the ELF basin V(H1,B1) which has a population of 1.97 electrons. The next feature to notice is again an interaction of Li with both nitrogen centers, basins V(N1,Li) = 2.0 electrons and V(Li,N2) = 2.9 electrons. In the latter, a larger population of almost three electrons can be found. This results in a smaller distance between N–Li, namely 1.846 Å compared to 2.043 Å in the previous case.

The electron distribution also shows that the B–N and the N–Li bonds, as described by the basins V(Li,N2) and V(N2,B2), both have a populations of ∼2.9 electrons, meaning they each have almost

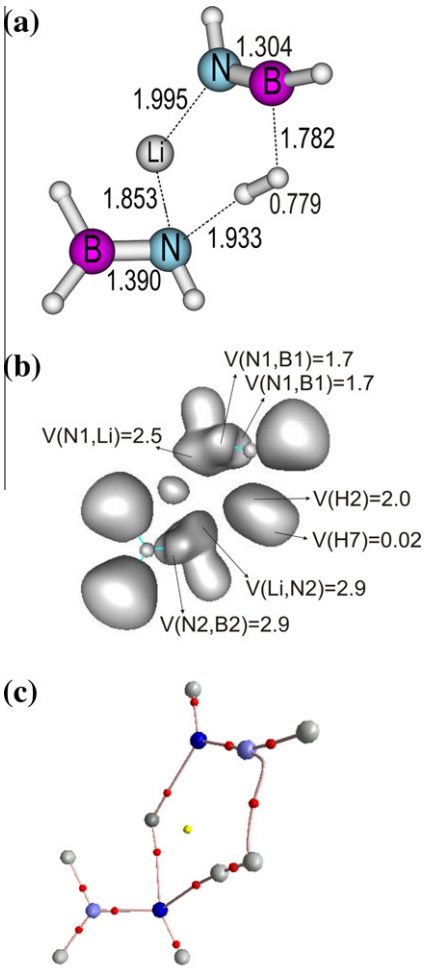

Figure 7. Structure analysis of **ts-3h2-1**: (a) selected geometrical parameters, (b) ELF basins including populations of some important basins, and (c) AIM map. All analyses are based on MP2/aVTZ optimized structure.

three electrons. N2 has 2 core electrons and five valence (V) electrons. One of the V-electrons is used in the H–N bond, two in the B–N bond, and the rest of two electrons are put in the N–Li bond. Thus, the free electron pair of nitrogen is spread over two bonds. The five V-electrons of N1 are arranged in a completely different manner. There are two V-electrons in N–H bonds, one V-electron in a B–N bond, and then the free electron pair of nitrogen is used to make a bonding between N1 and Li. Such an electron distribution makes the B1–N1 and N1–Li bonds longer than the B2–N2 and N2–Li bonds. It also suggests that a ring formation again occurs in this TS, which is confirmed by the AIM map showing ring critical point. Both TSs result in the same product, a complex between NH_2BH_2 and $LiNHBH_2$ with a relative energy of −2.3 kcal/mol.

3.4. Pathway for release of the third H_2 molecule

The associated energy profiles are displayed in Figure 6. From **bh2bh2–linhbh2** two TS for H_2 release are located. In **ts-3h2-2**, the H_2-lossis expected to occur from the monomer $LiNH_2BH_3$, and a high energy barrier of 67.5 kcal/mol. This TS gives rise to the product **bnh2nh2–linbh** with a relative energy of 15.2 kcal/mol. A lower energy barrier of 39.7 kcal/mol results from **ts-3h2-1** in which one H of one monomer interacts with another H of the other monomer.

A detailed description of the electronic reorganization can be found in Figures 7(a–c). Again, H_2 is practically formed, with a H–H distance is 0.779 Å, and the corresponding basin V(H2) = 2.0 electrons, and V(H7) = 0.02 electron. Lithium forms a chemical bond with both nitrogen's creating thus a cyclic adduct which ultimately stabilizes the TS. The latter TS leads to the $BH_2NHBHNHLi$ product with a relative energy of −12.2 kcal/mol.

3.5. Gibbs energy profiles

The effects of entropy and temperature on the course of a reaction can be evaluated from the relevant Gibbs (free) energy profiles. Figure 8 illustrates the lowest Gibbs energy pathways for hydrogen release from **ab–liab** at $T = 298$ K. Values are evaluated using the energies obtained at the MP2/aVTZ level in conjunction with the ZPE and entropy (S) values obtained at the MP2/avDZ level. In first instance, the Gibbs energy is higher than the previously described enthalpy counterparts. However when the first H_2 molecule is released, the Gibbs energy becomes lower. The more H_2 molecules are released the larger the difference between the enthalpy and Gibbs free energy becomes. This is however logical because the entropic contributions become larger when more separated molecules are formed. Perhaps more important is the fact that the barrier heights are not much changed on the Gibbs scale with respect to the enthalpic values, being between 1.5 and 3.4 kcal/mol.

Another point to notice is that the reaction becomes more exothermic by the addition of entropy, especially for the release of the third H_2. If the reaction could be stopped after the release of the second H_2 (which could be possible due to the higher energy of the corresponding TS), when starting from the separated reactants, while the reaction is exothermic by an enthalpy −21.7 kcal/mol, it remains exothermic in terms of free (Gibbs) energy, but by only −2.3 kcal/mol. If starting from the initial adduct, the reaction enthalpy amounts to −11.1 kcal/mol, whereas the reaction Gibbs energy suggests a nearly thermoneutral process.

This means that it could be more favored to regenerate the starting products. If needed, further studies are necessary on this topic but it goes beyond the scope of the present study.

4. Conclusions

In this Letter we investigate with the aid of reliable quantum chemical methods (MP2 and CCSD(T) with large one-electron basis) the mechanism for the hydrogen release reaction from a combination of $LiNH_2BH_3$ and NH_3BH_3 compounds. Our results reveal that release of one H_2 molecule requires an activation energy of ∼24 kcal/mol, the second H_2 release requires ∼26 kcal/mol, and the third ∼40 kcal/mol. The energy barrier for the release of the first H_2 molecule turns out to be lower than the barrier heights for the same processes from the monomers **ab** and **liab**, or from their dimers **2ab** and **2liab**. This can be rationalized by the effects of one Li substitution in **2ab**. This Li element tends to stabilize the initial complex, and because only one Li atom is present, formation of a dihydrogen bridge is still possible in the starting complex which in turn facilitates H_2 formation. The analysis of the electron distribution in the relevant transition structures show that formation of a pre-association cyclic adduct can be regarded as a responsible factor for the low energy barrier. This clearly demonstrates that the combined **ab–liab** system has even more potential as a hydrogen storage material than the separate **ab** or **liab**.

Acknowledgement

The authors thank the K.U. Leuven Research Council (GOA, IDO, PDM, IUAP programs) for continuing support.

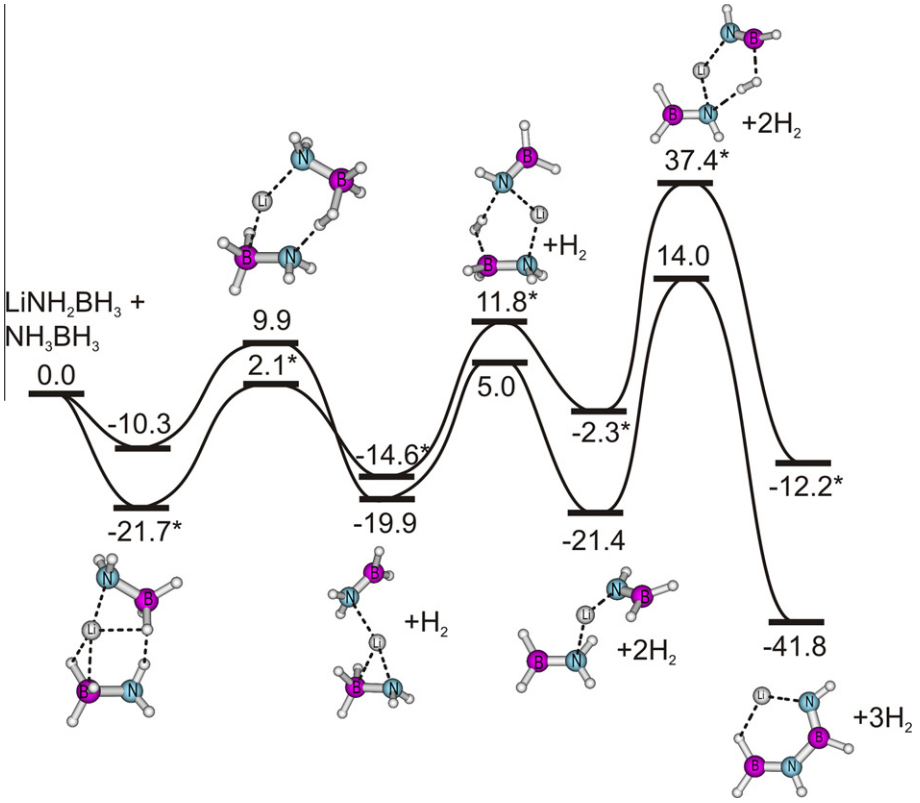

Figure 8. Lowest Gibbs energy profile for H_2 release from **ab**–**liab**. Gibbs energies at temperature T = 298.15 K are derived from total energies at the MP2/aVTZ level; zero-point energy (ZPE) and entropy (S) are obtained from MP2/aVDZ calculations.

Appendix A. Supplementary data

Supplementary data associated with this article can be found, in the online version, at doi:10.1016/j.cplett.2011.10.010.

References

[1] D.K. Ross, Vacuum 80 (2006) 1084.
[2] D.A.J. Rand, R.M. Dell, Hydrogen Energy: Challenges and Prospects, Royal Soc. Chem., Cambridge, 2008.
[3] M. Dressalhaus, G. Crabtree, M. Buchanan, Basic Energy Needs for the Hydrogen Economy, Office of Science, U.S. Department of Energy, Washington, DC, 2003.
[4] C.R. Miranda, G. Ceder, J. Chem. Phys. 126 (2007) 184703.
[5] F.H. Stephens, R.T. Baker, M.H. Matus, D.J. Grant, D.A. Dixon, Ang. Chem. Int. Ed. 46 (2007) 746.
[6] M. Bowden, T. Autrey, I. Brown, M. Ryan, in: Proceedings of 3rd International Conference on Advanced Materials and Nanotechnology, 2007, p. 498.
[7] J.B. Yang, J. Lamsal, Q. Cai, W.J. James, W.B. Yelon, Appl. Phys. Lett. 92 (2008) 091916.
[8] W.T. Klooster, T.F. Koetzle, P.E.M. Sigbahn, B.R. Richardson, R.H. Crabtree, J. Am. Chem. Soc. 121 (1999) 6337.
[9] A.C. Stowe, W.J. Shaw, J.C. Linehan, B. Schmid, T. Autrey, Phys. Chem. Chem. Phys. 9 (2007) 1831.
[10] F.H. Stephens, V. Pons, R. Tom Baker, Dalton Trans. (2007) 2613.
[11] M. Sana, G. Leroy, Int. J. Quant. Chem. 48 (1993) 89.
[12] Q.S. Li, J.G. Zhang, S.W. Zhang, Chem. Phys. Lett. 404 (2005) 100.
[13] J.G. Zhang, S.W. Zhang, Q.S. Li, J. Mol. Struct. Theochem. 717 (2005) 33.
[14] M.R. Weismiller, A.C.T. van Duin, J. Lee, R.A. Yetter, J. Phys. Chem. A 114 (2010) 5485.
[15] A. Staubitz, A.P.M. Robertson, I. Manners, Chem. Rev. 110 (2010) 4079.
[16] M.T. Nguyen, V.S. Nguyen, M.H. Matus, G. Gopakumar, D.A. Dixon, J. Phys. Chem. A 111 (2007) 679.
[17] V.S. Nguyen, M.H. Matus, D.J. Grant, M.T. Nguyen, D.A. Dixon, J. Phys. Chem. A 111 (2007) 8844.
[18] E. Mayer, Inorg. Nucl. Chem. Lett. 9 (1973) 343.
[19] A.C. Stowe, W.J. Shaw, J.C. Linehan, B. Schmid, T. Autrey, Phys. Chem. Chem. Phys. 9 (2007) 1831.
[20] C.W. Yoon, L.G. Sneddon, J. Am. Chem. Soc. 128 (2006) 13992.
[21] Z.T. Xiong et al., Nat. Mater. 7 (2008) 138.
[22] S. Swinnen, V.S. Nguyen, M.T. Nguyen, Chem. Phys. Lett. 489 (2010) 148.
[23] C.Z. Wu, G.T. Wu, Z.T. Xiong, X.W. Han, H.L. Chu, T. He, P. Chen, Chem. Mater. 22 (2010) 3.
[24] W. Li et al., J. Phys. Chem. C 114 (2010) 19089.
[25] M.J. Frisch, G.W. Trucks, et al., Gaussian 09, Revision A.1, Gaussian, Inc., Wallingford CT, 2009.
[26] H.-J. Werner, P.J. Knowels, et al., (Molpro, version 2006.1).
[27] J.A. Pople, R. Seeger, R. Krishnan, Int. J. Quant. Chem. Symp. 11 (1977) 149.
[28] T.H. Dunning, J. Chem. Phys. 90 (1989) 1007.
[29] R.A. Kendall, T.H. Dunning, R.J. Harrison, J. Chem. Phys. 96 (1992) 6796.
[30] D.E. Woon, T.H. Dunning, J. Chem. Phys. 98 (1993) 1358.
[31] G.D. Purvis, R.J. Bartlett, J. Chem. Phys. 76 (1982) 1910.
[32] K. Raghavachari, G.W. Trucks, J.A. Pople, M. Head-Gordon, Chem. Phys. Lett. 157 (1989) 479.
[33] C. Gonzalez, H.B. Schlegel, J. Chem. Phys. 90 (1989) 2154.
[34] R.F.W. Bader, Atoms in Molecules: A Quantum Theory, Clarendon Press, Oxford, 1995.
[35] P. Popelier, Atoms in Molecules An Introduction, Prentice hall, Harlow, England, 2000.
[36] A.D. Becke, K.E. Edgecombe, J. Chem. Phys. 92 (1990) 5397.
[37] S. Noury, F. Krokidis, F. Fuster, B. Silvi, TopMod Package, Universite Pierre et Marie Curie, Paris, 1998.
[38] L.J. Laaksonen, J. Mol. Graph. 10 (1992) 33.